PHILOSOPHICAL TRANSACTIONS OF THE ROYAL SOCIETY A MATHEMATICAL, PHYSICAL & ENGINEERING SCIENCES

A Review of Models of the Solar Photosphere and Low Chromosphere: The Temperature-Height Profile

D. L. Lambert

Phil. Trans. R. Soc. Lond. A 1971 **270**, 3-21
doi: 10.1098/rsta.1971.0055

Phil. Trans. Roy. Soc. Lond. A. **270**, 3–21 (1971) [3]
Printed in Great Britain

I. PHOTOSPHERE AND LOW CHROMOSPHERE

A review of models of the solar photosphere and low chromosphere: the temperature–height profile

By D. L. Lambert
Department of Astronomy, University of Texas, Austin, Texas, U.S.A.

Empirical and theoretical models of the photosphere and low chromosphere are reviewed with especial reference to the Bilderberg continuum atmosphere. The observations and analysis of the continuous spectrum are emphasized. A minimum electron temperature of 4300 K at $\lg\tau_0 \approx -4$ is suggested by new observations in the ultraviolet and far infrared.

1. Introduction

The solar photosphere and low chromosphere may be defined as the regions of the solar atmosphere in which the temperature is less than 9000 K. The deeper photospheric layers with $T \gtrsim 9000$ K are inaccessible to direct observation. The temperature rise through the chromosphere is probably severe above the height corresponding to $T \approx 9000$ K and, therefore, this transition region between the chromosphere and corona is not discussed in this paper. Athay (1969) shows that the coronal pressure provides a strict boundary condition for a model chromosphere; the temperature $T = 10\,000$ K must be reached within 2000 km above the limb. The deepest observable layers are about 300 km below the surface. This paper is devoted to a discussion of models to represent these 2300 km of the solar atmosphere.

A complete model would specify the magnitude and height variation of all significant variables; e.g. temperature, gas density, electron pressure, magnetic field and the velocity fields. The model would also include a representation of the spatial and temporal properties of the observable inhomogeneities, e.g. granulation, supergranulation and the chromospheric fine structures.

The emphasis throughout this review is on empirical derivations of the temperature–height relation. Pure theoretical models are discussed briefly in § 5. *The Bilderberg continuum atmosphere* (Gingerich & de Jager 1968) is an empirical model which may be adopted as a convenient reference model against which the more recent observational and theoretical results may be set. The abbreviation B.c.a. is adopted.

The majority of published measurements of the solar continuous spectrum have been obtained under conditions in which direct information on the fine scale structures is lost. Thus, the numerous empirical models in the literature were constructed as a representation of average conditions in the solar atmosphere. Direct observational studies of the fine scale features (e.g. granulation) are discussed in § 6. An empirical model is based upon a set of near standard assumptions. The atmosphere is considered to be composed of homogeneous plane-parallel layers which are in hydrostatic equilibrium. It is widely supposed that a condition of local thermodynamic equilibrium (l.t.e.) exists throughout the atmosphere.

These assumptions provide the fundamental integral equation relating the emergent continuous intensity $I_\lambda(0,\theta)$ to the temperature distribution $T(\tau_\lambda)$ in the atmosphere

$$I_\lambda(0,\theta) = \int_0^\infty B_\lambda(T(\tau_\lambda)) \exp(-\tau_\lambda \sec\theta) \sec\theta \, \mathrm{d}\tau_\lambda. \quad (1)$$

A standard notation is adopted. Here $B_\lambda(T)$ is the Planck function, λ is the wavelength, τ_λ is the optical depth and θ is the angle between the line of sight and the normal.

Observations of the intensity $I_\lambda(0, \theta)$ can be separated into two classes: absolute intensity (or spectral irradiance) measurements and limb darkening (or brightening) measurements, where

$$\phi_\lambda(\theta) = I_\lambda(0, \theta)/I_\lambda(0, 0)$$

is the limb darkening (or brightening) ratio. The distinction is a practical one based on the considerable simplification of observing procedure which results when relative intensities are sought.

Observations at a single wavelength determine $T(\tau_\lambda)$ over a restricted range of optical depth. The Eddington–Barbier relation $I_\lambda(0, \theta) \approx B_\lambda(\tau_\lambda = \cos\theta)$ illustrates the problem. Limb darkening observations from an average site can be obtained to a disk position $\cos\theta \gtrsim 0.2$. Then $T(\tau_\lambda)$ is reasonably well defined within the region $0.05 < \tau_\lambda < 2.0$. The mapping of $T(\tau_\lambda)$ at smaller optical depths can be achieved by extending the observations closer to the limb; e.g. observing at a site with exceptional seeing, or measuring the limb intensity distribution during total solar eclipse. An alternative method is to observe the intensity distribution at a wavelength such that the ratio of the continuous absorption coefficients $\kappa_{\lambda_1}/\kappa_{\lambda_2}$ (hence, also, $\tau_{\lambda_1}/\tau_{\lambda_2}$) differs significantly from unity (figure 1).

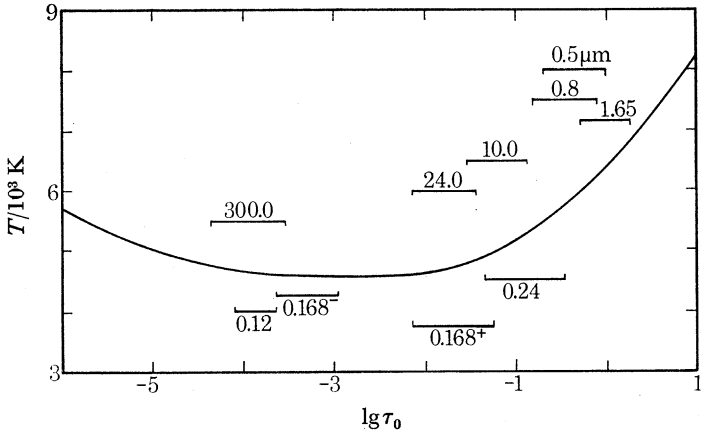

FIGURE 1. The temperature–optical depth relation for the *Bilderberg continuum atmosphere*. The horizontal lines indicate the region of the atmosphere between $\tau_\lambda = 1$ and $\tau_\lambda = 0.2$. The wavelength in micrometres is shown above the horizontal lines.

The derivation of $T(\tau_{\lambda_0})$, where λ_0 is a chosen standard wavelength, requires an identification and evaluation of the continuous opacity sources in the solar atmosphere. The conversion of optical depth τ_{λ_0} to geometrical height h is achieved through an integration of the equation of hydrostatic equilibrium. The notation $\tau_{\lambda_0} \equiv \tau_0$ and $\lambda_0 = 500\,\text{nm}$ is adopted.

The integral equation (1) can be solved by a trial and error procedure. A $T(\tau_0)$ relation with adopted absorption coefficients κ_λ/κ_0 is selected and the predicted intensities are compared with the observed values. The discrepancies are scrutinized and $T(\tau_0)$ adjusted accordingly. Other methods are discussed in the literature; Delache (1966) describes a general method of solution.

2. A NOTE ON THE CONTINUOUS ABSORPTION COEFFICIENT

The continuous absorption coefficient must be known in order that observations at two wavelengths may be converted to a single temperature distribution $T(\tau_0)$. The method of direct numerical integration of equation (1) from a given model requires that κ_λ/κ_0 be specified.

The dominant opacity source in the visible and infrared is provided by bound–free and free–free transitions of the negative hydrogen ion. Neutral hydrogen must be considered at the higher temperatures. Minor contributions are provided by the H_2^+ ion, He^-, bound–free absorption in the abundant elements (C, Mg, Si, Al, Fe), and Rayleigh and Thomson scattering.

Theoretical calculations of the H^- absorption coefficients have converged in recent years. The most recent calculations are provided by Geltman (1962, 1965), John (1964) and Doughty & Fraser (1966). Laboratory measurements of the bound–free cross-section were reported by Branscomb & Smith (1955) and Smith & Burch (1959). The agreement between theory and experiment is satisfactory. The most recent calculations of the free–free absorption coefficient are in good agreement and an accuracy of $\pm 10\,\%$ is indicated.

The dominant opacity sources in the ultraviolet are the bound–free (photoionization) contributions from the 'metal' elements. The photoionization cross-sections for the important elements have been determined from laboratory measurements and calculations.

Travis & Matsushima (1968) applied the quantum defect method to calculate cross-sections for N, O, Na, Mg, Al and Si. They show that the calculations are in reasonable agreement with the available measurements. They also tabulate the cross-sections for Cr, Fe and Ni which are obtained with the hydrogenic approximation. This approximation, and the recent upward revision of the solar photospheric iron abundance, indicate that iron may be an important opacity source between 250 and 170 nm. A laboratory determination or an improved calculation for iron would be welcomed. The metal opacities used in the prediction of intensities for the B.c.a. are discussed by Gingerich & Rich (1968) with their Fortran codes listed by Carbon & Gingerich (1969).

Collisionally induced absorption by H^- is not a significant contributor; Watson (1970) recalculated the cross-sections and showed that the earlier calculations (Weinberg & Berry 1966, 1968) provided gross overestimates. Drake (1970) has shown that a second state ($2p^2\,{}^3P$) of H^- is a bound state with an electron affinity of 0.0095 eV. It is unlikely that this state provides a significant contribution to the continuous opacity.

The proposal that the resonance broadened wings of Lyman-α could provide a significant contribution to the total absorption coefficient even at 400 nm was shortlived; Sando, Doyle & Dalgarno (1969) showed that the application of the conventional formula for the absorption coefficient in the extreme wing results in a gross overestimate. They conclude that the Lyman-α wings are unimportant longward of 200 nm.

The emergent radiation between about 500 and 2500 nm is produced by a common region of the photosphere. This overlap allows an assessment of the uncertainty in the absorption coefficient. Numerical evaluation shows that the limb darkening is independent of the choice for the H^- absorption coefficients. This result is readily attributable to the form of the $T(\tau_0)$ relation (Lambert 1968). Therefore, information on the absorption coefficients has to be extracted from the absolute intensity measurements. With an adopted uncertainty of $\pm 3\,\%$ the for absolute intensity $I_\lambda(0, 0)$, the equivalent uncertainty in the free–free absorption coefficient $\alpha_\lambda(H^-)_{f.f.}$ is estimated (Lambert 1965) at:

λ/μm	1.0	1.3	1.5	2.0	2.5
$\Delta\alpha_\lambda/\alpha_\lambda$ (%)	± 60	45	25	25	25

The best available measurements (see §3.1.2) can be reproduced by a model which predicts the observed limb darkening and absolute intensities throughout the interval ($0.7 < \lambda < 10\,\mu$m)

provided that the recent H^- absorption coefficients are adopted (Geltman 1962; John 1964; Doughty & Fraser 1966).

The older and less accurate calculations (Chandrasekhar & Breen 1946; Ohmura 1964) may also be rejected on the basis of the solar data (Lambert 1965, and unpublished calculations).

The effect of uncertainties in the bound–free cross-sections was also investigated (Lambert 1965). An uncertainty of $\pm 3\,\%$ in the absolute intensities corresponds to the following uncertainties in the ratio $r_\lambda = \sigma_\lambda/\sigma_0$ of the bound–free cross-sections.

λ/μm	0.6	0.8	1.0	1.2	1.4
$\Delta r_\lambda/r_\lambda$	± 5	± 10	± 15	± 20	± 25

This uncertainty is considerably greater than that resulting from the laboratory measurements.

More accurate absolute intensity measurements will be required before the analysis can seriously challenge the uncertainty estimates for the current H^- absorption coefficients. However, the above test suggests that their adoption for $\lambda > 2.5\,\mu$m should be satisfactory; the emergent intensity beyond 2.5 μm is emitted from progressively higher layers and the ratio κ_λ/κ_0 is required in order to relate $T(\tau_\lambda)$ to $T(\tau_0)$.

3. Observations of the solar continuous spectrum

An empirical model is developed from observations and, therefore, a survey of the observations of the solar continuous spectrum is an essential part of this review; the impact of the post-1968 observations on the B.c.a. is discussed in a later section.

Available absolute and relative observations of the continuous spectrum will be summarized. The results obtained following the Bilderberg Conference are given especial mention. It is noteworthy that a majority of the new results has been gathered by instruments aboard aircraft, balloons, rockets and satellites.

3.1. *The absolute intensity of the continuous spectrum*

3.1.1. *Introductory remarks*

Two useful quantities may be distinguished. The absolute intensity at the centre of the solar disk will be written $I_\lambda(0, 0)$. The measurement is made with a finite spectral bandpass and, hence, a correction for the Fraunhofer line absorption is required. The second quantity is the extra-terrestrial spectral irradiance H_λ, which is the incident energy per unit area per unit wavelength at the Earth's mean distance from the Sun. The total irradiance is also known as the solar constant. The relation between H_λ and $I_\lambda(0, 0)$ is discussed by Labs & Neckel (1968).

3.1.2. *The wavelength interval* 300 *to* 2500 nm

The observations available to the Bilderberg conferees were extensive for the interval 300 nm to 2.5 μm. However, independent measurements of $I_\lambda(0, 0)$ or H_λ were in poor agreement and systematic errors were demonstrably affecting most measurements. Since the independent check on the absorption coefficient calculations is based upon absolute intensity observations, a review of recent progress appears pertinent.

An excellent review (Labs & Neckel 1968) of the literature on absolute intensity and irradiance measurements is now available. These authors present tables of their recommended intensities, spectral irradiance and calibration factors for the *Göttingen* (Brückner 1960) and the *Utrecht Atlases* (Minnaert, Mulders & Houtgast 1940) of the Fraunhofer line spectrum.

PHILOSOPHICAL TRANSACTIONS OF THE ROYAL SOCIETY A MATHEMATICAL, PHYSICAL & ENGINEERING SCIENCES

The primary recommendations for $I_\lambda(0, 0)$ and H_λ are based upon the results of a thorough observational study (Labs & Neckel 1962, 1963, 1967). Their observations, which were obtained at the Jungfraujoch Scientific Station, provide the total absolute intensity $I_\lambda(0, 0)$ within well-defined passbands ($\Delta\lambda = 2.00$ or 2.05 nm. 169 measurements were made to map the spectrum between 329.0 and 654.9 nm at approximately 2 nm intervals. An additional 27 measurements were made in windows between 661.1 and 1246 nm. A standard tungsten filament lamp was used as the reference source. The accuracy of solar intensity measurements considered on a relative basis is claimed to exceed $\pm 1\,\%$. The accuracy of the absolute measurements is determined by the uncertainties in the standard lamp calibration: an uncertainty of $\pm 2\,\%$ at 500 nm is suggested. All previous measurements of $I_\lambda(0, 0)$ or the solar constant were scrutinized and reasons for their rejection were advanced.

Planimetry of the *Göttingen* and *Utrecht Atlases* was undertaken in order to convert the 2 nm integrals to a supposed continuum intensity. A calibration of the highest points in each Atlas scan is given in their paper. These points were considered to represent the continuum level and were compared with the normalized B.c.a. predicted intensities; the normalization—a slight increase in temperature—was made so that the predicted and observed intensities were in agreement at 500 nm. A discrepancy below 450 nm is discussed in § 4.

The relative intensity measurements by Pierce (1954) were adopted by Labs & Neckel in order to extend the $I_\lambda(0, 0)$ tabulation beyond their cut-off at 1250 nm. The relative values were scaled to give a best fit to the predicted intensities from the normalized B.c.a. The differences between the adjusted measurements and the predictions were within the expected uncertainty except at the short wavelength limit $1.0 < \lambda < 1.1\,\mu$m. New measurements confirm this normalization procedure.

Two important series of spectral irradiance measurements were made using instrumentation flown to an altitude of about 12 km aboard the National Aeronautics and Space Administration (Nasa) CV-990 aircraft. A spectroradiometer was operated by a group from the Nasa Ames Research Centre (Arvesen, Griffin & Pearson 1969). An in-flight calibration was made against a secondary standard of spectral irradiance. The spectral irradiance extrapolated to zero air-mass was mapped at high resolution within the interval $300\,\text{nm} < \lambda < 2.5\,\mu$m. An internal consistency of about $\pm 1\,\%$ was achieved; the absolute intensity errors are $\pm 5\,\%$ at 300 nm and $\pm 3\,\%$ throughout the visible and infrared.

A team from the Goddard Space Flight Center (G.S.F.C) (Thekaekara, Kruger & Duncan 1969) participated in the CV-990 flights. Four instruments were operated for spectral irradiance measurements but only two were satisfactorily calibrated against standard sources. The instruments were two monochromators (ranges 0.3 to 1.6 μm and 0.3 to 4 μm), a filter radiometer (0.3 to 1.1 μm) and a polarization interferometer (0.3 to 2.6 μm). The accuracy of the averaged values for the spectral irradiance is estimated at $\pm 5\,\%$.

The two new series of measurements are in reasonable agreement with the tabulations prepared by Labs & Neckel. This is shown in figures 2 and 3. The discrepancies are within the quoted uncertainties with the exception of a few wavelength intervals. Both series give higher radiances below about 500 nm. J. C. Arvesen (1970, personal communication) suggests that this disagreement will be reduced when a recently discovered error in the calibration of the spectral irradiance standard (Waters & Kostowski 1969) is taken into account. This correction will also reduce by a small percentage the total irradiance obtained by integration of their measurements; the corrected value will be close to the value obtained from recent radiometer experiments. These two

PHILOSOPHICAL TRANSACTIONS OF THE ROYAL SOCIETY A MATHEMATICAL, PHYSICAL & ENGINEERING SCIENCES

series of absolute measurements are in excellent agreement with the Labs & Neckel values between 1.0 and 2.5 μm. They confirm the latter's adoption of the model predictions for this interval.

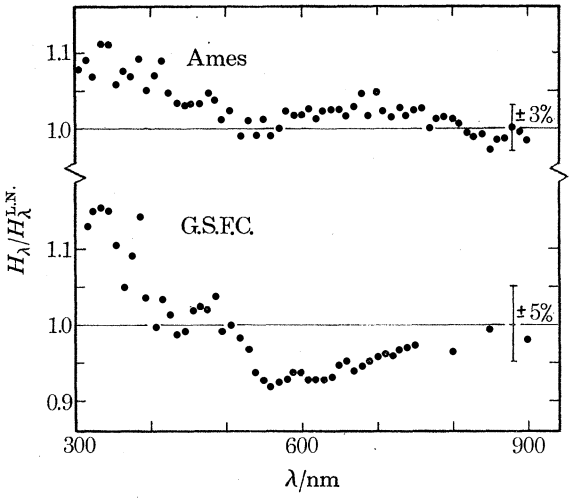

FIGURE 2. A comparison of recent spectral irradiance measurements and the results tabulated by Labs & Neckel (1968).

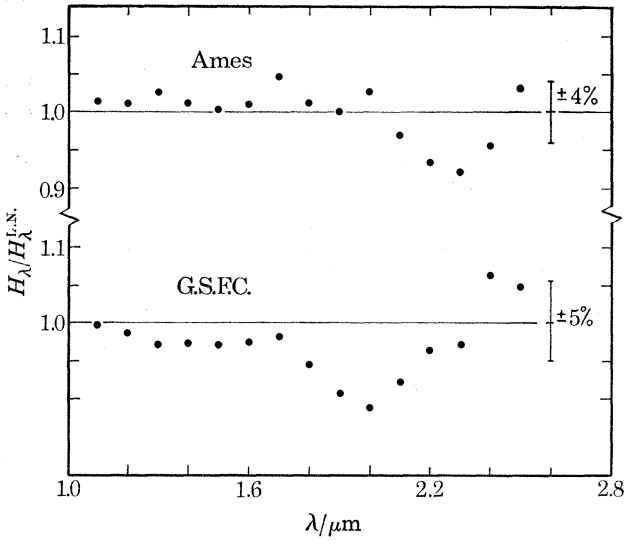

FIGURE 3. Recent spectral irradiance measurements for the wavelength interval $1.0 < \lambda < 2.5$ μm are compared with the results tabulated by Labs & Neckel (1968).

New measurements of the total irradiance or solar constant provide an additional check on the Labs & Neckel tabulations. Their result for the total irradiance was $S = 0.1365\,\mathrm{W\,cm^{-2}}$. Recent direct measurements using total radiometers flown to high altitude include

$$S = 0.1361 \pm 0.0014\,\mathrm{W\,cm^{-2}}$$

(Laue & Drummond 1968), and $S = 0.1351 \pm 0.0028\,\mathrm{W\,cm^{-2}}$ (Thekaekara *et al.* 1969) from four independent radiometers aboard the CV-990. The spectral irradiance results are in good agreement with these results. Since the two techniques use quite different radiometric standards, it is improbable that a systematic error exceeding 2 or 3 % can remain in the measurements of H_λ

and $I_\lambda(0, 0)$. This conclusion is not applicable to wavelength intervals ($\lambda \lesssim 350$ nm and $\lambda \gtrsim 2\ \mu$m) which contribute a minor percentage to the total irradiance.

3.1.3. *The wavelength interval* 2.5 *to* 25 μm

The interval 2.5 to 25 μm contains several windows through which observations have been obtained from the ground. More extensive observations have been made from aircraft and balloons. The results provided by Labs & Neckel are model atmosphere predictions but they noted the good agreement with the few available measurements in the 3 to 5 μm and 8 to 13 μm windows (Murcray, Murcray & Williams 1964; Farmer & Todd 1964; Saiedy 1960; Saiedy & Goody 1959).

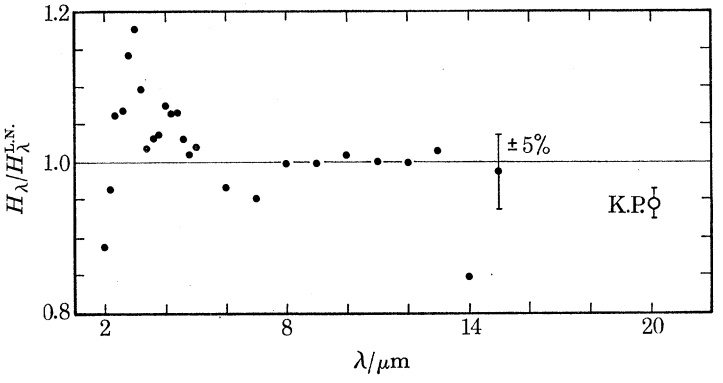

FIGURE 4. The spectral irradiances reported by Thekaekara *et al.* (1969) for the wavelength interval $2 < \lambda < 15\ \mu$m are compared with the normalized model predictions given by Labs & Neckel (1968). The intensity measurement $I_\lambda(0, 0)$ at 20.15 μm (Koutchmy & Peyturaux 1968) is also shown.

A more recent measurement at 20.15 μm was reported by Koutchmy & Peyturaux (1968). The equivalent brightness temperature at the centre of the disk is $T = 4590 \pm 110$ K, which is 5 % below the model prediction.

The G.S.F.C. (Thekaekara *et al.* 1969) instrumentation included a monochromator operating to 4 μm and a Michaelson interferometer for the interval 2.6 to 15 μm. The spectral radiance was measured from 2.5 to 15 μm with an accuracy of ± 5 %. The recent measurements are compared with the model predictions in figure 4. The agreement is excellent except below 4.5 μm;† the reasons for this latter discrepancy are not known. An instrumental origin can be suspected because the model predictions cannot be so severely adjusted.

3.1.4. *The wavelength interval* 25 μm *to* 1 cm

The Earth's atmosphere is opaque from the ground between about 25 μm and 1 mm. The continuous opacity increases as the square of the wavelength and this interval spans the large part of the solar atmosphere in which the temperature reaches a minimum value. Newly reported measurements are discussed in this section.

The solar brightness temperature between 238 and 312 μm was measured by Eddy, Léna & MacQueen (1969*a*). A Michelson interferometer (Eddy, Lee, Léna & MacQueen 1970) was flown in the Nasa CV-990 aircraft at a maximum altitude of nearly 13 km. The Sun was observed at a fixed elevation, and therefore the standard Langley plots could not be made. Instead, the

† The discrepant point at 14 μm is possibly attributable to a misprint in table 3 presented by Thekaekara *et al.* (1969).

transmission of the atmosphere was calculated from theoretical spectra including H_2O, N_2 and O_2 absorption lines (Eddy, Léna & MacQueen 1969*b*). The authors argue that this calculation provides an accurate estimate of the transmission. However, the transmission in an adjacent interval 333 to 500 μm is anomalously weak and an unidentified terrestrial absorber is believed to be present. Thus, more complete observations are required in order to check the transmission calculations in the 238 to 312 μm interval. The mean brightness temperature is $T = 4370 \pm 260$ K between 328 and 312 μm.

Balloon observations (altitude 25 to 28 km) were reported by Gay *et al.* (1968). An interferometer mapped the solar spectrum between 50 and 200 μm. The reported brightness temperature $T \simeq 5500$ K at about 60 μm decreases to $T = 4600$ K between 100 and 200 μm. Their high brightness temperature at 60 μm is inconsistent with other evidence and their results are rejected.

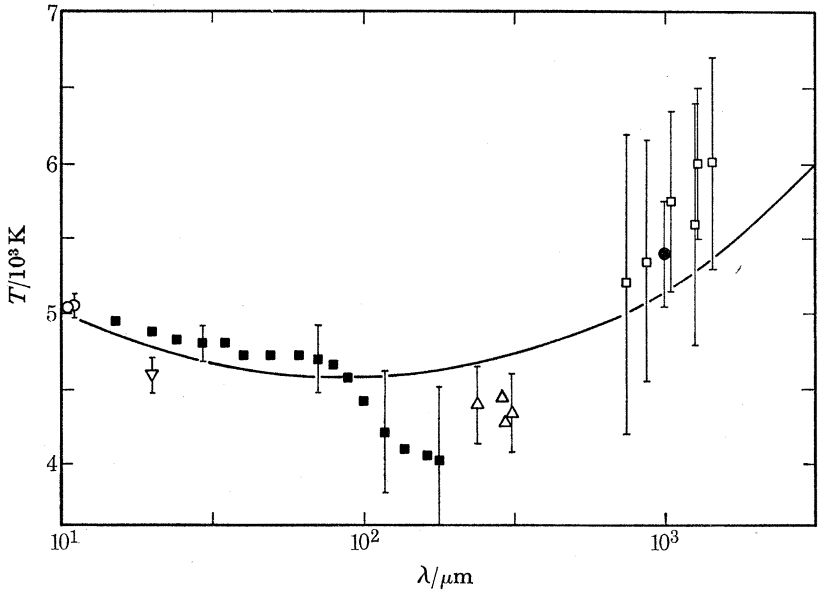

FIGURE 5. The brightness temperature T_λ for the wavelength interval $10 < \lambda < 1000$ μm. The B.c.a. predictions are shown by the solid line. The measurements, which are discussed in the text, are denoted by the following symbols: ○, Saiedy (1960); ■, Mankin & Strong (1970); ▽, Koutchmy & Peyturaux (1968); △, Eddy Léna & MacQueen (1969*a*); □, Fedoseev, Lubyako & Kukin (1968); ●, Low & Gillespie (1969).

Relative measurements have been reported by Beer (1966) and Mankin & Strong (1970). Beer obtained a relative intensity distribution between 21 and 43 μm, which is consistent with the B.c.a. predicted intensities (Labs & Neckel 1968). Mankin & Strong made limb darkening measurements at six wavelengths between 11 and 115 μm. The balloon-borne instrument package was operated at 27 km. Although relative intensities were measured, the results at the different wavelengths were linked together because the the λ^2 dependence of the H^- absorption coefficient and the Rayleigh–Jeans approximation result in the identity:

$$T(\lambda, \sec\theta) = T(\lambda_*, \sec\theta_*), \tag{2}$$

where $\lambda^2 \sec\theta = \lambda_*^2 \sec\theta_*$. The results (figure 5) were normalized to the brightness temperature at 11 μm (Saiedy & Goody 1959).

The wavelength interval 300 to 750 μm remains unexplored. Extensive observations longward of 1 mm are summarized by Shimabukuro & Stacey (1968).

Brightness temperature measurements for the interval $25\,\mu\text{m} < \lambda < 2\,\text{mm}$ are compared in figure 5 with the B.c.a. predictions. The points near 1 mm are the most recent measurements. A comparison with older data is given by Noyes, Beckers & Low (1968) and Simon & Zirin (1969). The temperature rise beyond 1 mm reaches $T = 9100 \pm 200\,\text{K}$ at $\lambda = 2\,\text{cm}$ (Buhl & Tlamicha 1969) and, hence, the emission beyond 2 cm comes from layers above the low chromosphere.

3.1.5. *The ultraviolet* $\lambda < 300\,\text{nm}$

Observations in this wavelength interval are obtained with instruments carried in rockets or satellites. Some significant new results have been published since the Bilderberg Conference.

Newer measurements of $I_\lambda(0, 0)$ with an uncertainty $\pm 30\,\%$ are reported by Bonnet (1968) (figure 6). Stigmatic spectra with a resolution of 0.04 nm were obtained and central intensity measurements made in regions which were free from strong Fraunhofer lines. The observations were in the interval $290 < \lambda < 300\,\text{nm}$.

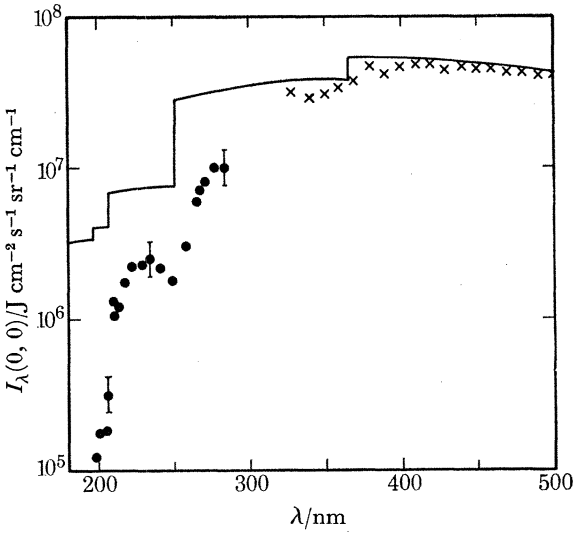

FIGURE 6. The absolute intensity at the centre of the disk for the wavelength interval $200 < \lambda < 500$ nm. The solid line is the predicted intensity distribution according to the model proposed by Holweger (1967). The B.c.a. predictions are very similar. The observations (×) for $\lambda > 300$ nm are a sample of the intensity measurements by Labs & Neckel (1968) which represent possible windows between Fraunhofer line absorption. The data points (●) for $\lambda < 300$ nm are taken from Bonnet (1968) and are subject to the indicated 30 % uncertainty.

The choice of the temperature minimum ($T = 4600\,\text{K}$) in the B.c.a. was influenced by the minimum colour temperature obtained near 165 nm. Newly reported measurements show a marked disagreement.

Widing, Purcell & Sandlin (1970) provide absolute intensities $I_\lambda(0, 0)$ in the interval 208 to 145 nm which were obtained from photographic spectra with a resolution of about 0.02 nm. The lowest brightness temperature occurs at 166.5 and 168.2 nm, where $T = 4670 \pm 50\,\text{K}$. These new results are in good agreement with earlier results obtained by the same group. In the interval 208 to 198 nm, there is good agreement with Bonnet (1968).

Results obtained from a photoelectric scanning spectrometer with a resolution of 6 pm are reported by Parkinson & Reeves (1969). Continuum intensities were measured in 19 windows between 198.4 and 283.9 nm. These absolute intensities $I_\lambda(0, 0)$ are a factor of three lower than

the values given by Widing *et al.* Hence, the minimum brightness temperature is lower by about 250 K. This discrepancy is considerable and additional observations are required.

Preliminary absolute intensities for the interval $150 < \lambda < 90$ nm are reported by Gingerich (1970 and personal communication). These OSO-IV results are in good agreement with the rocket results of Parkinson & Reeves. The brightness temperature ranges from 5400 to 5600 K and, therefore, the radiation is produced by the low chromosphere.

Observations (spectra and spectoheliograms) of the Lyman continuum (Noyes & Kalkofen 1969) have been obtained with OSO-IV. These observations provide information on the temperature and density distribution at the top of the low chromosphere.

3.2. *Observations of the centre-limb variations*

A considerable body of data is available on centre-limb variations in the continuum; Holweger (1967), Elste (1968) and Sauval (1968) provide references to this literature. Brief comments are given here.

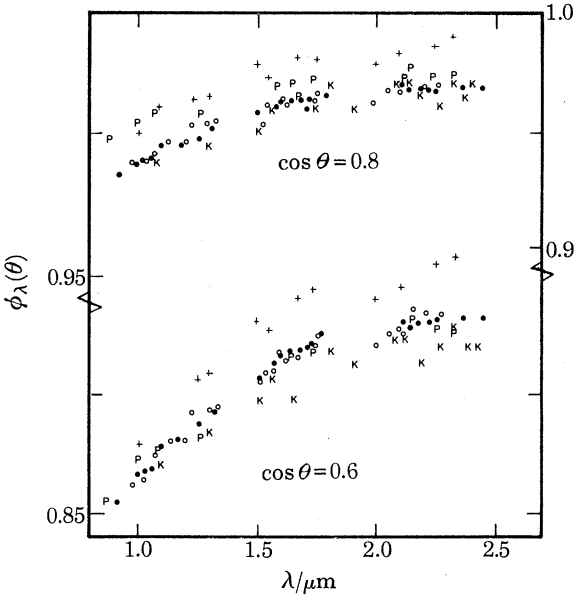

FIGURE 7. Limb darkening observations for the wavelength interval $1.0 < \lambda < 2.5$ μm and the disk positions as $\cos\theta = 0.8$ and 0.6. +, Peyturaux (1952); P, Peyturaux (1955); ●, Pierce (1954) as corrected by David & Elste (1962); ○, Lambert (1965); K, Kozhevnikov (1957).

The wavelength interval 300 nm to 2.5 μm has been the most intensively studied. The standard limb darkening measurements are those provided by Pierce (1954) as corrected by David & Elste (1962). These may be supplemented in the ultraviolet by the results of Peyturaux (1955). Lambert (1965) measured the limb darkening at 30 wavelengths between 1 and 2.5 μm. The results for the disk positions $\cos\theta \geqslant 0.2$ are in excellent agreement with the values given by David & Elste (1962). Other series of measurements (Peyturaux 1952, 1955; Kozhevnikov (1957) may be rejected (see figures 7 and 8).

Limb darkening observations have been made in the atmospheric windows beyond 2.5 μm. A recent study (Léna 1970) included measurements at 5, 10 and 20 μm and disk positions $1 \geqslant \cos\theta \geqslant 0.06$. Mankin & Strong (1970) describe centre-limb scans at 18, 31, 52, 83 and 115 μm (see § 3.1.4). No limb brightening was reported by either Léna or by Mankin & Strong. No

observations are yet available for the interval 115 μm $< \lambda <$ 1 mm. Limb brightening is reported at the extreme limb at 1 mm (Noyes *et al.* 1968; Newstead 1969). Observations between 1 mm and 2 cm also show the intensity distribution to be flat (Simon & Zirin 1969). A sharp intensity spike at the extreme limb was discovered in observations at $\lambda = 8.6$ mm obtained during a total solar eclipse (Coates 1958). This must be a general feature of the centre-limb variation in this wavelength range.

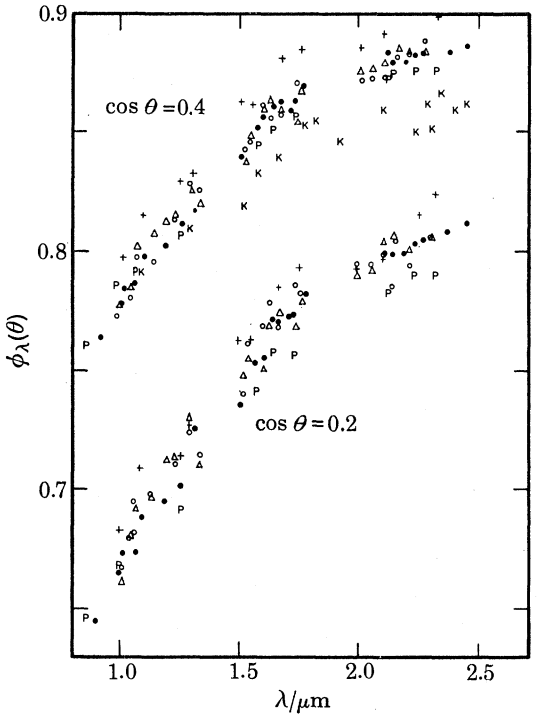

FIGURE 8. Limb darkening observations for the wavelength interval $1.0 < \lambda < 2.5$ μm and the disk positions $\cos\theta = 0.4$ and 0.2. The key to the symbols is given in the legend of figure 7. The diagram includes a second series of measurements (△) observed by Lambert (1965). The two series are distinguished by the rates (○, diurnal rate; △, a slow drift rate) at which the Sun was allowed to drift across the entrance aperture of the spectrometer.

The limb darkening is observed to be increasing between 500 and 320 nm, which is the atmospheric cut-off. The increase continues into the ultraviolet. Bonnet (1968) gives the intensity distribution at 21 wavelengths between 283.9 and 194.6 nm. The increase continues until $\lambda = 230$ nm, and then remains approximately unchanged between 230 and the Al I discontinuity at 207 nm; it is considerably less severe below 207 nm. Shortward of 200 nm, the limb darkening continues to decrease. The disk brightness is approximately neutral between about 155 and 165 nm. Shortward of 155 nm, limb brightening is observed (Tousey 1963). Good quantitative measurements of the centre-limb variation for $\lambda < 190$ nm are not yet available.

4. Empirical models

Can an empirical model reproduce the observed continuous spectrum? The answer is no. It is important to indicate how closely a model atmosphere may reproduce the observations. The B.c.a. provides a convenient reference model.

One objection to the B.c.a. is a trivial one: the model does not reproduce either the observed absolute intensity distribution near 500 nm or the limb darkening observations in the visible and near infrared. The method of construction of the composite model was responsible for this error. The correction is realized by increasing the temperatures and temperature gradient below $\tau_0 = 1$. However, the goodness of fit to the limb darkening observations raises several questions.

The radiation in the interval 500 nm to 2.5 μm is emitted by essentially identical layers. Therefore, one may expect to determine a unique $T(\tau_0)$ distribution responsible for the absolute intensities and the limb darkening observations. A comprehensive attempt was made by Lambert (1965) who concluded that no single $T(\tau_0)$ relation provided a satisfactory reproduction of the observations.† A good compromise was developed and presented at the Bilderberg Conference. This temperature distribution with the best absorption coefficient data (see § 2) gave a satisfactory fit to the observed continuous spectrum within the interval 700 nm $< \lambda <$ 10 μm. The predicted and observed limb darkening diverged for wavelengths shortward of 700 nm. A similar result was found by Holweger (1967, Figure 3*a*). Rather poor agreement with the absolute intensities in the infrared was reported by Holweger (1967) and Sauval (1968), but this disagreement is entirely attributable to their derivations of the mean observed $I_\lambda(0, 0)$ values from a mass of apparently conflicting observations. It should be noted that no empirical addition to the continuous absorption coefficient is required for this spectral region. The temperature gradient may be increased to improve the fit with the limb darkening observations at around 500 nm but this must introduce slight discrepancies at other wavelengths. Since the model predictions were obviously in disagreement with the observations for $\lambda \lesssim 450$ nm, a slight discrepancy in limb darkening for $\lambda < 700$ nm and $\cos\theta = 0.2$ was considered acceptable and was attributed to the unknown effects operating at the shorter wavelengths. The possible sources of error are (i) an error in the observed limb darkening, (ii) an unidentified opacity source, and (iii) the failure of a single $T(\tau_0)$ relation to adequately represent the inhomogeneities (granulation).

The uncertainties in the limb darkening observations are probably too small to account for the discrepancy. However, it can be noted that the original observations by Pierce (1954) are quite consistent with the model (see also Holweger 1967, Figure 3*a*). The discrepancy occurs between the corrected observations (David & Elste 1962) and the predictions. A limb darkening measurement at $\lambda = 589.3$ nm by Mattig & Schröter (1961), which was corrected for scattered light according to the procedure discussed by David & Elste, disagrees with the interpolated David & Elste values and is in good agreement with the predictions. A remeasurement of limb darkening in the visible region would be of some interest.

Below about 450 nm, the discrepancies between the model predictions and the absolute intensities are considerable. Labs & Neckel rediscussed this problem and tentatively suggested that the supposed windows between Fraunhofer lines were substantially depressed by numerous weak and overlapping lines. Holweger (1970) examined nine windows. He computed the continuum depression resulting from the wings of nearby strong lines and, in addition, he searched through laboratory line lists and estimated the equivalent widths of all lines occurring within the window. He was able to show that the total line absorption was sufficient to depress his computed continuum intensities into agreement with the Labs & Neckel intensity calibration of the window (see figure 9). The calculations showed that a window at 500.9 nm was depressed by about 2.5 % on account of weak lines. This depression should be taken into account in fitting model predicted intensities to the observations at 500 nm. The difference is equivalent to a 40 K

† The recent observations reviewed in § 3 reinforce the 1965 conclusions.

PHILOSOPHICAL TRANSACTIONS OF THE ROYAL SOCIETY A MATHEMATICAL, PHYSICAL & ENGINEERING SCIENCES

adjustment in temperature. The identification of the Fraunhofer line contribution also slightly improves the agreement with the limb darkening observations. The residual discrepancy is probably attributable to the influence of inhomogeneities.

Longward of 2.5 μm, the free–free absorption of H^- has a limiting λ^2 dependence. This increase means that increasingly higher layers of the atmosphere contribute to the radiation. Hence, new observational data for $\lambda > 2.5\,\mu$m can be interpreted with an adjustment of the model for the outer layers. The B.c.a. was constructed with a broad temperature minimum $T = 4600$ K centred on $\log \tau_0 = -3.0$. The brightness temperature measurements between 25 μm and 1 mm (figure 5) indicate that the temperature minimum might be decreased by 100 to 200 K. However, the evidence from this region alone cannot be considered to demand such a reduction.

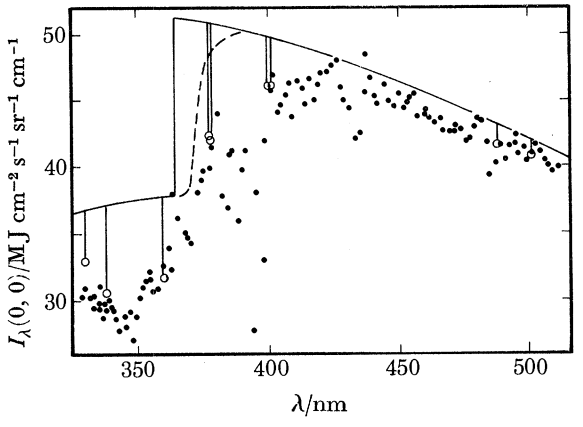

FIGURE 9. The intensity distribution for the continuous spectrum in the wavelength interval $330 < \lambda < 510$ nm (after Holweger 1970). The predicted intensities for the Holweger model are shown by the solid line. The predicted intensities in nine windows are shown by the open circles and include the estimated Fraunhofer line absorption (see text). The broken line is an estimate of the continuum depression produced by overlapping Balmer lines. The observed intensities (filled circles) from Labs & Neckel (1968) are the highest points from scans in the *Göttingen* and *Utrecht Atlases*.

The increasing temperature for $\lambda \gtrsim 1$ mm reflects the chromospheric temperature rise. The opacity source is free–free transitions in hydrogen and it also has a λ^2 dependence; hence the brightness temperature is predicted to be a function of $\lambda^2 \sec\theta$ for a spherically symmetric model. However, Simon & Zirin (1969) show that the available observations at millimetre wavelengths indicate a flat intensity distribution to at least $0.8R_\odot$. Fine scale chromospheric structure must be responsible for the absence of the limb brightening predicted by the idealized model.

The observations in an interval $170 \lesssim \lambda \lesssim 300$ nm are only in moderate agreement with the predicted intensities (Bonnet 1968, and figure 6). The origin of this discrepancy is unclear; it could be considered an extension of the smaller discrepancies in the interval $300 < \lambda < 500$ nm. Bonnet (1968) assumed that the problem lay in a missing opacity source. He derived the approximate wavelength and temperature dependence of the unidentified absorber. The intensity predictions for the revision of the B.c.a. derived by Gingerich (1969, 1970) also show discrepancies with the observations. Clearly, it would be of interest to extend into the ultraviolet Holweger's calculations of the predicted line absorption in selected windows.

The calculations provide intensity discontinuities (figure 10) which include $\lambda = 251$ nm (Mg I), $\lambda = 207.1$ nm (Al I), $\lambda = 168$ nm (Si I). The predicted magnitude of the former two edges is approximately consistent with the observations. The latter edge, where the B.c.a. and revised

B.c.a. predict an intensity decrease of at least a factor of ten, is just perceptible in the observations (Parkinson & Reeves 1969; Widing *et al.* 1969). The next absorption edge $\lambda = 152.5$ nm (Si I) is not observed and this absence is predicted by the B.c.a. revision while the B.c.a. predicts a slight intensity increase. The edges shortward of 160 nm are observed and predicted to be in emission.

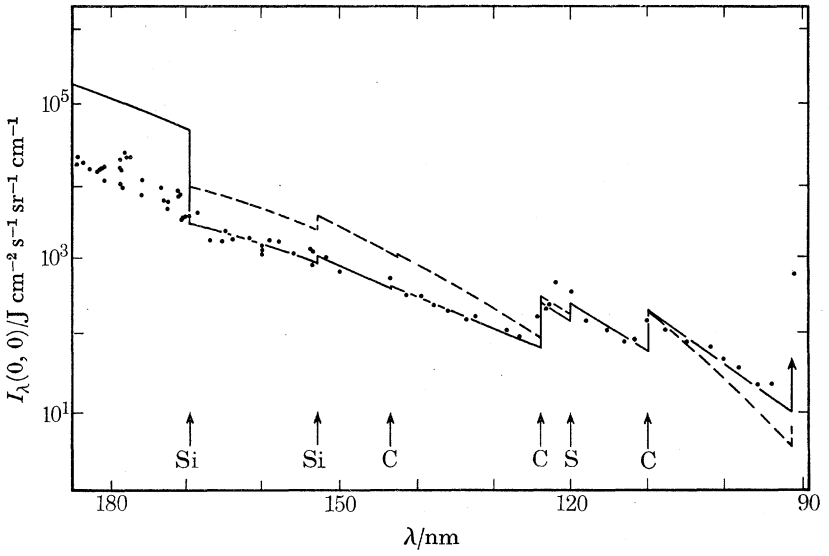

FIGURE 10. The absolute intensity distribution in the wavelength interval $90 < \lambda < 180$ nm (after Gingerich 1970). The predicted intensities are shown for the B.c.a. (broken line for $\lambda \leqslant 170$ nm) and for the revised B.c.a. (solid line) discussed by Gingerich. The B.c.a. predicted intensity just shortward of the Si I edge at 168 nm is $\lg I_\lambda(0, 0) = 6.0$. The revised B.c.a. predictions include the opacity contribution from the resonance broadened Lyα wing. The conventional formula was used to estimate this opacity and its contribution is probably over-estimated for $\lambda \gtrsim 170$ nm (Sando, Doyle & Dalgarno 1969).

The weak intensity discontinuity at 168 nm suggests that either the temperature minimum be extended to larger optical depths or that there is an unidentified opacity source in this region. The predicted limb darkening for the B.c.a. and revised B.c.a. is in qualitative agreement with the observed transition from limb darkening to limb brightening with the neutral region at about 160 nm.

The temperature rise through the chromosphere according to the B.c.a. and revised B.c.a. atmospheres was adjusted to fit ultraviolet intensities shortward of about 160 nm and the observed brightness temperatures at millimetre wavelengths. The two regions of the spectrum require similar temperature distributions but exact agreement cannot be expected on account of fine scale structures.

At the wavelength corresponding to the minimum brightness temperature, the disk is approximately uniformly bright. With the absence of significant limb brightening (or darkening), the minimum electron temperature must be close to the minimum brightness temperature. The temperature derived from the ultraviolet intensities depends on the observations selected; the lower temperature $T \approx 4300$ K is obtained with the intensities reported by Parkinson & Reeves (1969). The temperature minimum $T \approx 4300$ K is consistent with the analyses of Ca II, H and K profiles; e.g. Avrett & Linsky (1970). It is also the predicted boundary temperature for the line blanketed non-l.t.e. model (Athay 1969).

Recently proposed models are compared in figure 11. Heintze's (1969) tentative model is not consistent with the observations, e.g. the brightness temperature measurements between 50 and

300 μm. The other models are very similar for $\log \tau_0 \gtrsim -4$ and the differences reflect the weights given by the authors to various parts of the spectrum: e.g. the lower temperatures required by Léna's model appear to result from normalization of his 20 μm limb darkening results to the absolute intensity reported by Koutchmy & Peyturaux (1968) which is somewhat below the predicted intensities for the other models.

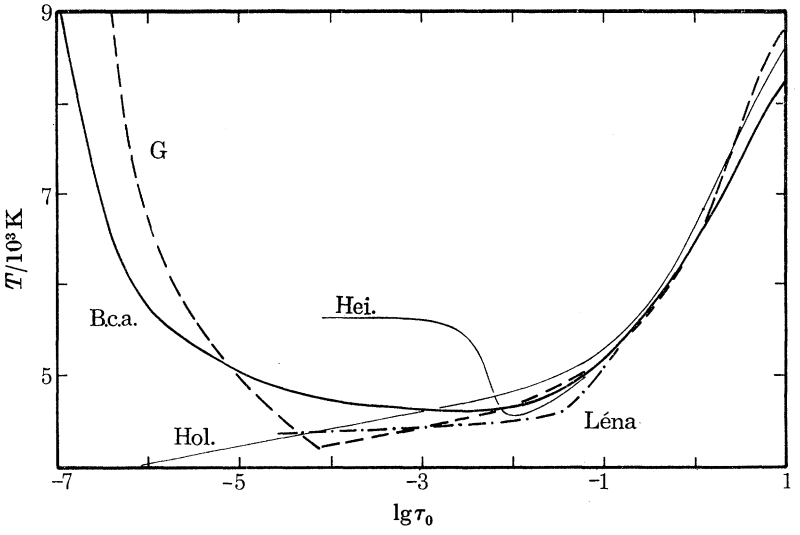

FIGURE 11. The $T(\tau_0)$ relations for selected models. The models are: B.c.a., Bilderberg continuum atmosphere; G, revised B.c.a. (Gingerich 1970); Hol., Holweger (1967); Hei., Heintze (1969); Léna, Léna (1970).The $T(\tau_0)$ relation for the model Hei. is shown only to $\lg \tau_0 = -1$. Holweger (1967) gave the temperature distribution as a function of the Rosseland mean optical depth $\bar{\tau}$, it is assumed $\bar{\tau} = \tau_0$.

The chromospheric rise is the least well-defined portion of the model but the B.c.a. revision must be approximately correct (see § 6). The absence of limb brightening at the millimetre wavelengths can only be explained by an inhomogeneous model of the low chromosphere. Also, Gingerich's revision of the B.c.a. assumes l.t.e. but non-l.t.e. effects must be considered.

The non-l.t.e. effects for hydrogen begin to be important above the temperature minimum; the analysis of the Lyman continuum observations (Noyes & Kalkofen 1969) takes them into account. Gingerich (1970) states that the Lyman continuum analysis indicates that the temperature in the low chromosphere is 200 to 300 K hotter than the B.c.a. revision with a reduction in temperature gradient at about $T = 7500$ K.

The model proposed by Holweger (1967) has a low boundary temperature $T = 3900$ K. The temperature distribution for $\log \tau_0 \lesssim -4$ is based on an analysis of line profiles of strong lines under the assumption that l.t.e. is valid. The temperature minimum has to be located now at about $\log \tau_0 = -4$. The line profiles can only be reconciled with the increasing temperature above this depth when the assumption of l.t.e. is discarded. The rejection of l.t.e. is reasonable.

5. THEORETICAL MODELS

The empirically determined temperature relation $T(\tau_0)$ provides an excellent test for model stellar atmosphere calculations. Comparisons of constant flux calculations with the observed $T(\tau_0)$ have shown that absorption line blanketing must be considered. A considerable effort has been directed toward providing an accurate treatment of the line blanketing.

Statistical treatments of line blanketing have been attempted; Carbon & Gingerich (1969) and Carbon (1969) report results obtained with the picket-fence approximation. With their triple picket models, they simulate the opacity contributions from the continuum, line cores and line wings. The relative weights for the three picket levels were assigned on the basis of the approximation that the blanketing within a particular wavelength interval can be represented by a set of equal and non-overlapping lines with doppler profiles. The dependence of line opacity with depth was considered in an approximate but adequate treatment. The spectrum was divided into five intervals and the total opacity contribution due to the lines in each interval was fixed by matching the computed and observed line blanketing coefficients.

The details of the triple picket-fence approximation and the method of solution for the constant flux atmosphere are given by Carbon & Gingerich (1969). The theoretical and revised B.c.a. $T(\tau_0)$ relations differ by less than 100 K for $\lg \tau_0 \gtrsim -1.2$. In the higher layers $\lg \tau_0 < -1.2$, the triple picket model shows a slow approach to the boundary temperature of about 4700 K.

A fourth picket level was introduced by Carbon (1969). This additional level was chosen to account for the strong Fraunhofer lines.† Quadruple picket calculations were performed; with the contributions of the fourth level computed according to either pure absorption or pure scattering. The pure absorption calculations gave a model which was in good agreement with the revised B.c.a. over a region extending to the temperature minimum; the predicted boundary temperature was $T \approx 4200$ K. The adoption of pure scattering for line formation in the fourth level resulted in a temperature distribution which was similar to the earlier triple picket calculation. An independent approach to a line blanketed model atmosphere was reported by Athay (1970). Six categories of lines were recognized; weak, medium-strong and strong lines from neutral and ionized metals. L.t.e. was not assumed. The self-consistent model has a boundary temperature $T = 4300 \pm 100$ K which is good agreement with the estimates from the ultraviolet and infrared observations.

The extension of the theoretical calculations to predict the temperature rise through the chromosphere is a problem for further study. A slight temperature increase can be attributed to n.l.t.e. effects in the H^- population (Cayrel 1963; see also Skumanich 1970). Feautrier (1968) constructed a constant-flux solar atmosphere in which n.l.t.e. effects for the H^- ion were included. This unblanketed model showed a temperature minimum $T = 4680$ K and a temperature plateau which was 500 K above the minimum temperature and extended outward from $\log \tau_0 \approx -6$. The observed temperature rise is much greater because of the significant heating contribution from mechanical sources.

6. Concluding remarks

In this review the recent observations of the solar continuous spectrum were examined and their impact on models of the photosphere and low chromosphere were discussed. Some important aspects of model construction were omitted and are briefly mentioned in this concluding section.

The Fraunhofer line spectrum is a key to many facets of the model. In addition to providing checks on the basic parameters of the model (e.g. temperature and pressures), the Fraunhofer lines yield information on the complex velocity fields (microturbulence, convective and

† The blanketing effect of the Balmer lines was treated separately in both the triple and quadruple picket calculations.

PHILOSOPHICAL TRANSACTIONS OF THE ROYAL SOCIETY A MATHEMATICAL, PHYSICAL & ENGINEERING SCIENCES

oscillatory velocities) and the inhomogeneities. The basic parameters of present models are consistent with observations of the weak or medium strong Fraunhofer lines; Holweger (1967) demonstrates this. The very strong lines (e.g. Ca II H and K) require a consideration of n.l.t.e effects. None the less, their impact on models may be very direct (Avrett & Linsky 1970).

The absolute intensity in the K I minima of the H and K lines corresponds to a radiation temperature of about 4300 K. If the chromosphere is optically thick at the line centre, the minimum electron temperature is equal to or less than 4300 K. A spirited argument developed during the Bilderberg Conference over the possibility that the chromosphere is optically thin at the line centres. Further study showed that the optical thin hypothesis was untenable. Thus, the analysts of the Ca II H and K profiles are happy with the reduction in the temperature minimum from B.c.a. value of 4600 to the 4300 K suggested by newer observations in the ultraviolet and far infrared.

No consideration was given in the review to the observations of the flash spectrum and the extreme limb intensities. The continuum emission at the extreme limb was discussed by Hiei & Faller (1968). The temperature profile which they derive is consistent with the revised B.c.a. For example, the temperature gradient within 200 km of the limb was estimated

$$\mathrm{d}(T^{-1})/\mathrm{d}r = a = (3 \pm 1) \times 10^{-12}\,\mathrm{cm}^{-1}\,\mathrm{K}^{-1}.$$

In the B.c.a. revision, the region from the temperature minimum $T = 4200$ K to 5000 K has a gradient $a = 1.8 \times 10^{-12}\,\mathrm{cm}^{-1}\,\mathrm{K}^{-1}$ which is in good agreement with the eclipse result. The gradient a decreases for $T \gtrsim 5000$ K and this is also required by the analyses of eclipse observations. The eclipse observations also provide a check on the densities in the low chromosphere. Henze (1969) interpreted slitless spectrograms of the Balmer lines and provided a preferred model for the heights 500 to 1200 km above the limb. He noted that the B.c.a. corresponded to lower temperatures by 1200 to 1900 K and lower electron densities by a factor of an order of magnitude at the greatest heights. Both discrepancies are essentially removed by the B.c.a. revision.

The present empirical models are unsuccessful in some areas. The discrepancies are probably related to the failure of the standard assumptions of homogeneous layers in hydrostatic and local thermodynamic equilibrium. Studies of n.l.t.e. effects are now a familiar part of the literature related to the chromosphere.

There is no doubt that the next crucial requirement for the models is to define the inhomogeneities. Preliminary studies of granulation are providing information on the temperature fluctuations in the photosphere. Wilson (1969*a*) has interpreted the centre-limb observations of the r.m.s. intensity contrast determined from Stratoscope photographs (Edmonds 1962) in terms of a r.m.s. temperature fluctuation $\Delta T_{\mathrm{r.m.s.}}$ which has a maximum $\Delta T_{\mathrm{r.m.s.}} = 600$ K at $\tau_0 \approx 0.8$ and a possible second maximum below $\tau_0 \approx 3$. Observations of the granulation in the continuum and Fraunhofer ('wiggly') lines over an extended wavelength interval are urgently required; Blamont & Carpentier (1968) obtained photographs in the ultraviolet $\lambda \approx 200$ nm and identified granulation. The ultraviolet observations are important owing to the possibility of defining the properties of the inhomogeneities within the region of the temperature minimum.

The important observational problems for future investigation include:

an accurate ($\Delta T = \pm 50$ K) mapping of the brightness temperature in the region 20 μm to 1 mm;

continuum and Fraunhofer line studies of the granulation with high spatial resolution ($\Delta\theta \simeq 0.1''$) in the visible and ultraviolet;

a study of the continuous spectrum between 180 and 300 nm to determine the opacity sources;

PHILOSOPHICAL TRANSACTIONS OF THE ROYAL SOCIETY A MATHEMATICAL, PHYSICAL & ENGINEERING SCIENCES

a new determination of the minimum brightness temperature near 165 nm;

centre-limb and absolute intensities below 165 nm;

a study of the complex chromospheric structure from spectra and spectroheliograms with excellent spatial resolution.

The solutions to these major problems will come from observations obtained above the Earth's atmosphere. As a result, current models of the photosphere and low chromosphere will develop in complexity and the solar physicist will be challenged to provide convincing physical interpretations.

I wish to thank Drs D. Carbon, O. Gingerich and E. M. Purcell for sending me their results in advance of publication, and Drs J. Arvesen, T. M. Kendall and M. P. Thekaekara for helpful conversations.

I am indebted to the Royal Society and the British National Committee on Space Research for the opportunity to present this paper at their discussion meeting.

References (Lambert)

Arvesen, J. C., Griffin, R. N. & Pearson, J. B. 1969 *Appl. Opt.* **8**, 2215.
Athay, R. G. 1969 *Solar Phys.* **9**, 51.
Athay, R. G. 1970 *Bull. Am. astr. Soc.* **2**, 181.
Avrett, E. H. & Linsky, J. 1970 *Bull. Am. astr. Soc.* **2**, 181.
Beer, R. 1966 *Nature, Lond.* **209**, 1226.
Blamont, J-E. & Carpentier, G. 1968 *Ann. d'Astrophys.* **31**, 333.
Bonnet, J. 1968 *Ann. d'Astrophys.* **31**, 597.
Branscomb, L. M. & Smith, S. J. 1955 *Phys. Rev.* **98**, 1028.
Brückner, G. 1960 Photometrischer Atlas des Nahen ultravioletten Sonnen spektrums 2988–3629 Å, Göttingen.
Buhl, D. & Tlamicha, A. 1969 *Astrophys. J.* **153**, L189.
Carbon, D. F. 1969 *Bull. Am. astr. Soc.* **1**, 337.
Carbon, D. F. & Gingerich, O. 1969 *Proc. 3rd Harvard-Smithsonian Conf. on Stellar Atmospheres*, p. 377.
Cayrel, R. 1963 *C. r. hebd. Séanc. Acad. Sci., Paris* **257**, 3309.
Chandrasekhar, S. & Breen, F. H. 1946 *Astrophys. J.* **104**, 430.
Coates, R. J. 1958 *Astrophys. J.* **128**, 83.
David, K-H. & Elste, G. 1962 *Z. Astrophys.* **54**, 12.
Delache, P. 1966 *Ann. d'Astrophys.* **29**, 109.
Doughty, N. A. & Fraser, P. A. 1966 *Mon. Not. R. astr. Soc.* **132**, 267.
Drake, G. W. F. 1970 *Phys. Rev. Lett.* **24**, 126.
Edmonds, F. N. 1962 *Astrophys. J.* (Suppl.) **6**, 367.
Eddy, J., Léna, P. J. & MacQueen, R. M. 1969*a* *Solar Phys.* **10**, 330.
Eddy, J., Léna, P. J. & MacQueen, R. M. 1969*b* *J. atmos. Sci.* **26**, 1318.
Eddy, J. A., Lee, R. H., Léna, P. J. & MacQueen, R. M. 1970 *Appl. Opt.* **9**, 439.
Elste, G. 1968 *Solar Phys.* **3**, 106.
Farmer, C. B. & Todd, S. J. 1964 *Appl. Opt.* **3**, 453.
Feautrier, P. 1968 *Ann. d'Astrophys.* **31**, 257.
Fedoseev, L. I., Lubyako, L. V. & Kukin, L. M. 1968 *Soviet Astr.* **11**, 953.
Gay, J., Lequeux, J., Verdet, J., Turon-Lacarrieu, P., Bardet, M., Roucher, J. & Zeau, Y. 1968 *Astrophys. Lett.* **3**, 169.
Geltman, S. 1962 *Astrophys. J.* **136**, 935.
Geltman, S. 1965 *Astrophys. J.* **141**, 376.
Gingerich, O. 1969 *Bull. Am. astr. Soc.* **1**, 277.
Gingerich, O. 1970 Preprint.
Gingerich, O. & de Jager, C. 1968 *Solar Phys.* **3**, 5.
Gingerich, O. & Rich, J. C. 1968 *Solar Phys.* **3**, 82.
Heintze, J. R. W. 1969 *Bull. Astr. Inst. Neth.* **20**, 137.
Henze, W. 1969 *Solar Phys.* **9**, 56, 65.
Hiei, E. & Faller, J. E. 1968 *Solar Phys.* **3**, 513.
Holweger, H. 1967 *Z. Astrophys.* **65**, 365.

PHILOSOPHICAL TRANSACTIONS OF THE ROYAL SOCIETY A MATHEMATICAL, PHYSICAL & ENGINEERING SCIENCES

Holweger, H. 1970 *Astr. & Astrophys.* **4**, 11.
John, T. L. 1964 *Mon. Not. R. astr. Soc.* **131**, 315.
Koutchmy, S. & Peyturaux, R. 1968 *C. r. hebd. Séanc. Acad. Sci., Paris* **267**, 905.
Kozhevnikow, N. I. 1957 *Soviet Astr.* **1**, 856.
Labs, D. & Neckel, H. 1962 *Z. Astrophys.* **55**, 269.
Labs, D. & Neckel, H. 1963 *Z. Astrophys.* **57**, 283.
Labs, D. & Neckel, H. 1967 *Z. Astrophys.* **65**, 133.
Labs, D. & Neckel, H. 1968 *Z. Astrophys* **69**, 1.
Lambert, D. L. 1965 Thesis, Oxford University.
Lambert, D. L. 1968 *Solar Phys.* **3**, 118.
Laue, E. G. & Drummond, A. J. 1968 *Science, N.Y.* **161**, 888.
Léna, P. 1970 *Astr. & Astrophys.* **4**, 202.
Low, F. J. & Gillespie, C. M. 1969 *Bull. Am. astr. Soc.* **1**, 199.
Mankin, W-G. & Strong, J. 1970 *Solar Phys.* (in the Press).
Mattig, W. & Schröter, E. H. 1961 *Z. Astrophys.* **52**, 195.
Minnaert, M., Mulders, G. F. W. & Houtgast, J. 1940 *Photometric atlas of the solar spectrum from* λ3613 *to* λ8771, Amsterdam: Schnabel.
Murcray, F. H., Murcray, D. G. & Williams, W. J. 1964 *Appl. Opt.* **3**, 1373.
Newstead, R. A. 1969 *Solar Phys.* **6**, 56.
Noyes, R. M., Beckers, J. M. & Low, F. J. 1968 *Solar Phys.* **3**, 36.
Noyes, R. W. & Kalkofen, W. 1969 *Bull. Am. astr. Soc.* **1**, 288.
Ohmura, T. 1964 *Astrophys. J.* **140**, 282.
Parkinson, W. H. & Reeves, E. M. 1969 *Solar Phys.* **10**, 342.
Peyturaux, R. 1952 *Ann. d'Astrophys.* **15**, 302.
Peyturaux, R. 1955 *Ann. d'Astrophys.* **18**, 34.
Pierce, A. K. 1954 *Astrophys. J.* **120**, 221.
Saiedy, F. 1960 *Mon. Not. Roy. astr. Soc.* **121**, 483.
Saiedy, F. & Goody, R. M. 1959 *Mon. Not. Roy. astr. Soc.* **119**, 213.
Sando, K., Doyle, R. O. & Dalgarno, A. 1969 *Astrophys. J.* **157** L, 443.
Sauval, A. 1968 *Solar Phys.* **3**, 89.
Shimabukuro, F. K. & Stacey, J. M. 1968 *Astrophys. J.* **152**, 777.
Simon, M. & Zirin, H. 1969 *Solar Phys.* **9**, 317.
Skumanich, A. 1970 *Astrophys. J.* **159**, 1077.
Smith, S. J. & Burch, D. S. 1959 *Phys. Rev.* **116**, 1125.
Thekaekara, M. P., Kruger, R. & Duncan, C. H. 1969 *Appl. Opt.* **8**, 1713.
Tousey, R. 1963 *Space Sci. Rev.* **2**, 3.
Travis, L. D. & Matsushima, S. 1968 *Astrophys.* **154**, 689.
Waters, W. R. & Kostowski, H. J. 1969 Abstract of paper read at October 1969 meeting of J.O.S.A.
Watson, W. D. 1970 *Phys. Rev.* **1** A (3rd Series), 4.
Weinberg, M. & Berry, R. S. 1966 *Phys. Rev.* **144**, 75.
Weinberg, M. & Berry, R. S. 1968 *Phys. Rev.* **165**, 334.
Widing, K. G., Purcell, E. M. & Sandlin, G. D. 1970 *Solar Phys.* **12**, 52.
Wilson, P. R. 1969*a* *Solar Phys.* **6**, 364.
Wilson, P. R. 1969*b* *Solar Phys.* **9**, 303.

PHILOSOPHICAL TRANSACTIONS OF THE ROYAL SOCIETY A MATHEMATICAL, PHYSICAL & ENGINEERING SCIENCES